



HAL
open science

Variance computation of MAC and MPC for real-valued mode shapes from the stabilization diagram

Szymon Gres, Michael Dohler, Palle Andersen, Laurent Mevel

► To cite this version:

Szymon Gres, Michael Dohler, Palle Andersen, Laurent Mevel. Variance computation of MAC and MPC for real-valued mode shapes from the stabilization diagram. IOMAC 2019 - 8th International Operational Modal Analysis Conference, May 2019, Copenhagen, Denmark. pp.1-9. hal-02143765

HAL Id: hal-02143765

<https://inria.hal.science/hal-02143765>

Submitted on 29 May 2019

HAL is a multi-disciplinary open access archive for the deposit and dissemination of scientific research documents, whether they are published or not. The documents may come from teaching and research institutions in France or abroad, or from public or private research centers.

L'archive ouverte pluridisciplinaire **HAL**, est destinée au dépôt et à la diffusion de documents scientifiques de niveau recherche, publiés ou non, émanant des établissements d'enseignement et de recherche français ou étrangers, des laboratoires publics ou privés.



IOMAC'19

8th International Operational Modal Analysis Conference
2019 May12-14 Copenhagen

VARIANCE COMPUTATION OF MAC AND MPC FOR REAL-VALUED MODE SHAPES FROM THE STABILIZATION DIAGRAM

Szymon Gres¹, Michael Döhler², Palle Andersen³, Laurent Mevel²

¹ Aalborg University, Department of Civil and Structural Engineering,
Thomas Manns Vej 23, 9000 Aalborg, Denmark

² Inria, Ifsttar, Univ. Rennes,
Campus de Beaulieu, 35042 Rennes, France

³ Structural Vibration Solutions A/S,
NOVI Science Park, 9220 Aalborg, Denmark

ABSTRACT

Recent advances in efficient variance computation of modal parameter estimates from the output-only subspace-based identification algorithms make the modal parameter variance a practical modal indicator, indicating the accuracy of the estimation. A further modal indicator is the Modal Assurance Criterion (MAC), for which a recently developed uncertainty quantification scheme estimates the variance at a fixed model order. The Modal Phase Collinearity (MPC) is another popular indicator, for which an uncertainty scheme is currently missing. Unlike other modal parameters, which are Gaussian distributed, estimates of MAC and MPC are close to the border of their respective distribution support and cannot be approximated as a Gaussian random variable. This paper addresses the respective uncertainty quantification of MAC and MPC. The results are validated in the context of operational modal analysis (OMA) of a spring mass system.

Keywords: uncertainty quantification, operational modal analysis, Modal Assurance Criterion, Modal Phase Collinearity, stabilization diagram

1. INTRODUCTION

In Operational Modal Analysis (OMA) the modal parameters, namely natural frequencies, damping ratios and mode shapes, are estimated based on modeling of a linear system that is identified from measurements. It involves only the output data, such as accelerations, displacements, velocities or strains,

recorded on the structure under some unknown, unmeasured, ambient excitation conditions. Estimates of the modal parameters are impaired with statistical uncertainties, since they are computed from data of finite length, which are usually also afflicted by noise. Hence, they are never equal to the true physical parameters of the structure, even if the assumed model is correct. Those uncertainties should be quantified or accounted for, which is often crucial in practice when interpreting the modal results.

In this context, first order perturbation theory is used to compute the variance of modal parameter estimates from the covariance-driven output-only stochastic subspace identification in [13], which is based on the developments of [11]. An efficient multi-order implementation of the latter scheme was derived in [4, 5]. This enabled the application of uncertainty quantification of the modal parameters in practical applications e.g. for computing the variance of natural frequencies, damping ratios and mode shapes estimated from bridge measurements [1, 2, 12]. The framework in [5] was extended to multi-setup subspace identification in [3]. Subsequently, the scheme for the uncertainty quantification of modal parameters was generalized to the family of input-output and output-only data-driven stochastic subspace identification methods in [9].

In the context of accounting for bias errors, the modal parameters can be clustered into so-called modal alignments by some practical criteria, like the relative difference between the parameters and the modal indicators. One modal alignment is a group of modal parameters that correspond to one theoretical mode and are estimated within a range of system orders. A group of modal alignments of some selected parameters, like the natural frequencies, is called a stabilization diagram. A strategy to compute the so called global modal parameters from the stabilization diagram was proposed in [1]. There, the global estimates of the modal parameters correspond to the means of the respective natural frequencies and the damping ratios at different modal orders, weighted with their statistical uncertainties. Like the estimates of the modal parameters computed at a single model order, the global estimates are stochastic variables thus their covariance and consequently the confidence bounds can be quantified, such as in [1].

The interpretation of the modal parameter estimates can be enhanced by the so-called modal indicators, which are quantities reflecting some physical aspects of the estimated mode shapes. Those indicators, Modal Assurance Criterion (MAC) and Modal Phase Co-linearity (MPC), inherit the statistical uncertainties from the underlying mode shape estimates. While the statistical framework for modal parameters is well-known and developed in the context of subspace-based system identification methods, uncertainty quantification of modal indicators has not been carried out yet. In this paper we address the uncertainty quantification of MAC and MPC computed for estimates of real-valued mode shapes obtained from the stabilization diagram.

2. BACKGROUND

In this section the underlying mechanical model is recalled and the statistical parameters of interest are defined.

2.1. Vibration modeling

Motion behavior of a viscously damped, linear time-invariant (LTI) structural system can be represented by a discrete-time stochastic state-space model

$$\begin{cases} x_{k+1} = A_n x_k + w_k \\ y_k = C_n x_k + v_k \end{cases} \quad (1)$$

where $x_k \in \mathbb{R}^n$ are the states, and $A_n \in \mathbb{R}^{n \times n}$, $C_n \in \mathbb{R}^{r \times n}$ are the state transition and observation matrices estimated at a model order n . Vectors w_k with v_k denote the process and output noises. The eigenfrequencies f_i , damping ratios ζ_i and mode shapes φ_i of the underlying mechanical system are

identified for $i = 1 \dots n$ from the i -th eigenvalue λ_i and eigenvector Φ_i of A_n such that

$$f_i = \frac{|\lambda_{ci}|}{2\pi}, \quad \zeta_i = \frac{-\Re(\lambda_{ci})}{|\lambda_{ci}|}, \quad \varphi_i = C_n \Phi_i \quad (2)$$

where every eigenvalue of the continuous system λ_{ci} is computed with $e^{\lambda_{ci}\tau} = \lambda_i$. The $|\cdot|$ denotes the modulus operator and $\Re(\cdot)$ and $\Im(\cdot)$ express the real and imaginary parts of a complex variable.

2.2. MAC computation

Let $\hat{\varphi}$ and $\hat{\psi}$ be two mode shapes estimated on N samples. As N goes to infinity both mode shape estimates converge almost surely to their respective true values φ_* and ψ_* . The MAC formulation between two complex valued mode shapes vectors φ and ψ follows [6] and writes

$$\text{MAC} = \frac{|\varphi^H \psi|^2}{\varphi^H \varphi \psi^H \psi} = \frac{\varphi^H \psi \psi^H \varphi}{\varphi^H \varphi \psi^H \psi}. \quad (3)$$

A consistent estimate of the MAC can be obtained by using consistent estimates of the mode shape vectors φ and ψ . In this paper we will investigate the computation of MAC between two mode shape estimates of the same mode obtained from a modal alignment.

When assuming $\hat{\varphi} = \hat{\psi}$, meaning that the two mode shapes of interest are co-linear, the MAC yields 1, which is a constant value with no statistical uncertainty. On the other hand when the two modes shapes of interest are orthogonal $\hat{\varphi}^H \hat{\psi} = 0$ the MAC yields 0, which is also a constant value with no statistical uncertainty. Based on that, the MAC indicator is bounded between 0 and 1, which makes its uncertainty assessment difficult, especially when the estimates of MAC approach their theoretical bounds. That is what is investigated in this paper.

2.3. MPC computation

The complexity of a vector can be quantified by the Modal Phase Collinearity (MPC) [7, 10]. By definition the MPC is expressed as

$$\text{MPC}(\varphi) \triangleq \frac{(\lambda_1 - \lambda_2)^2}{(\lambda_1 + \lambda_2)^2} \quad (4)$$

where λ_1 and λ_2 are the eigenvalues of matrix $\begin{bmatrix} S_{xx} & S_{xy} \\ S_{yx} & S_{yy} \end{bmatrix} \in \mathbb{R}^{2 \times 2}$, where $S_{xx} = \Re(\varphi)^T \Re(\varphi)$, $S_{yy} = \Im(\varphi)^T \Im(\varphi)$ and $S_{xy} = S_{yx} = \Re(\varphi)^T \Im(\varphi)$. The expression in (4) can be simplified to

$$\text{MPC}(\varphi) = \text{MAC}(\varphi, \bar{\varphi}) = \frac{(S_{xx} - S_{yy})^2 + 4(S_{xy})^2}{(S_{xx} + S_{yy})^2}, \quad (5)$$

which was established in [14]. Consequently, similar to the MAC, the MPC indicator computed from the data has some stochastic properties, that are functions of the stochastic properties of the mode shapes. Also, as well as the MAC, the MPC is bounded between 0 and 1, depending whether the mode shape of interest is respectively a purely imaginary or a purely real vector. The quantification of the statistical uncertainties of the estimates of the MPC is investigated in this paper.

2.4. Uncertainty quantification of modal parameters

Here we will set up some numerical simulation for which we will estimate the modal parameters and their underlying uncertainties. Consider a theoretical 6 DOF chain-like system that, for any consistent set of units, is modeled with a spring stiffness $k_1 = k_3 = k_5 = 100$ and $k_2 = k_4 = k_6 = 200$, mass $m_i = 1/20$ and a proportional modal damping matrix. The system is subjected to a white noise signal in

all DOFs and sampled with a frequency of 50Hz for 2000 seconds. The responses are measured at DOFs 1, 2 and 5. White Gaussian noise with a standard deviation equal to 5% of the standard deviation of the output is added to the response at each channel. The computations are performed in a Monte Carlo setup with $m = 1000$ simulations. Both the output-only data driven subspace-based system identification (SSI-UPC) and the variance computation in the corresponding framework based on [5] are set up with time lags of 15 and 200 blocks for the covariance computation of the data Hankel matrix. To compute the modal alignments and the stabilization diagram, the considered system orders are in the range between 12 and 40. Six global modes are determined, with their respective modal parameters and their variances, in each simulation. The confidence intervals of the global modal parameters are computed after [1]. For the formation of each modal alignment the following criteria are used

- difference in two consecutive natural frequencies $\leq 1\%$,
- difference in two consecutive damping ratios $\leq 10\%$,
- MAC level between two consecutive mode shapes $\geq 99\%$,
- standard deviation of natural frequency computed with perturbation theory $\leq 1\%$.

The results presented first are established based on one realization of the Monte Carlo simulations. Figure 1 illustrates the estimates of the natural frequency with the corresponding 95% confidence intervals computed for model orders 12 – 40 together with the estimates of the global natural frequency and its corresponding 95% confidence interval.

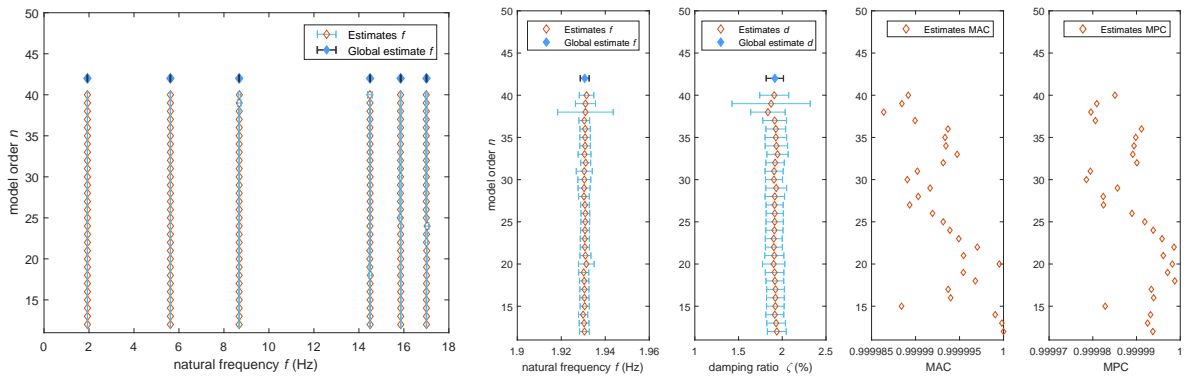


Figure 1: Stabilization diagram for natural frequencies with the corresponding 95% confidence intervals (left). Estimates of natural frequencies, damping ratios, MAC and MCF from the first modal alignment (right).

One can see that the natural frequency of each mode can be tracked along the system orders and the estimated variances are small, thus not visible in the scale presented on the Figure 1 (left). Subsequently, the dispersion of the natural frequencies, damping ratios and modal indicators is illustrated for the first modal alignment on Figure 1 (right). The fusion of the multi-order estimates of natural frequencies and damping ratios is reflected by the global estimates.

The variance of the modal parameter estimates computed with the Delta method based on one data set is reflected in the dispersion of the histogram of that parameter computed from the Monte Carlo simulations. This is illustrated in Figure 2 for the global estimates of the natural frequencies and damping ratios of the first mode and the estimates of the real and imaginary parts of the first DOF from the global mode shape corresponding to the first mode.

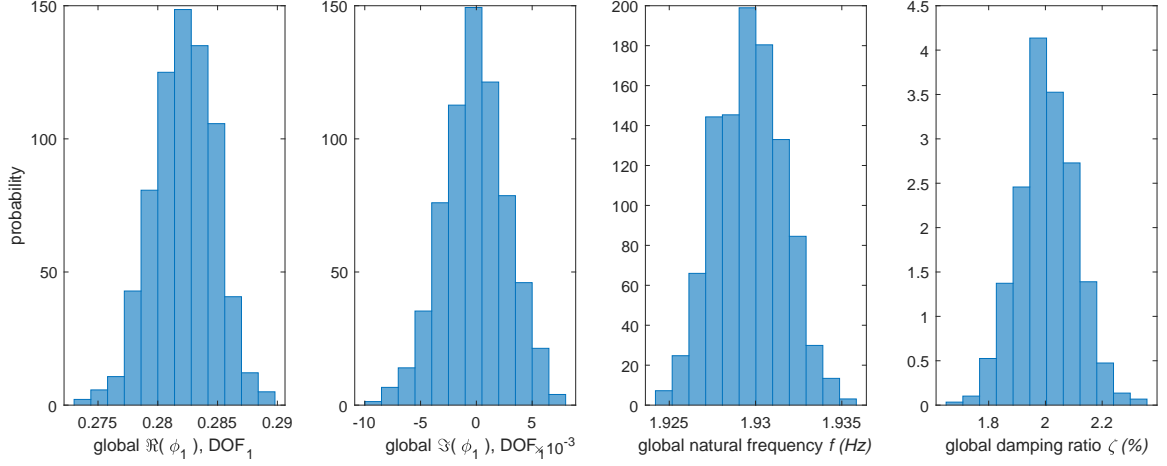


Figure 2: Histograms of the global estimates of modal parameters corresponding to the first mode based on Monte Carlo simulations. Respectively from the left: estimates of the real part of the global mode shape, the imaginary part of the global mode shape, global natural frequency and global damping ratio.

It can be observed that each histogram reflects some Gaussian distribution, which complies with the assumptions of the Delta method used in the Gaussian approximation of the modal parameter estimates. Additionally, confidence bounds of the global estimates of the natural frequency and damping ratio accurately encompass the area corresponding to the 95% quantile of the respective Monte Carlo histograms, which also validates the deployed theory.

2.5. Problem statement

Now we will illustrate how the distribution of the MAC and the MPC derived from the Monte Carlo histogram differs from the Gaussian distribution of the modal parameters when the considered mode shape estimates are asymptotically real-valued and selected from the same modal alignment. For that consider two cases of MAC and MPC, namely

1. $\text{MAC}(\hat{\varphi}^{1,12}, \hat{\psi}^{1,14})$ is computed between the mode shapes from the first modal alignment at model orders 12 and 14, namely $\hat{\varphi}^{1,12}$ and $\hat{\psi}^{1,14}$,
2. $\text{MPC}(\hat{\varphi}^{1,12})$ is computed for the mode shape corresponding to the first mode estimated at model order 12, namely $\hat{\varphi}^{1,12}$.

These distributions are illustrated on Figure 3.

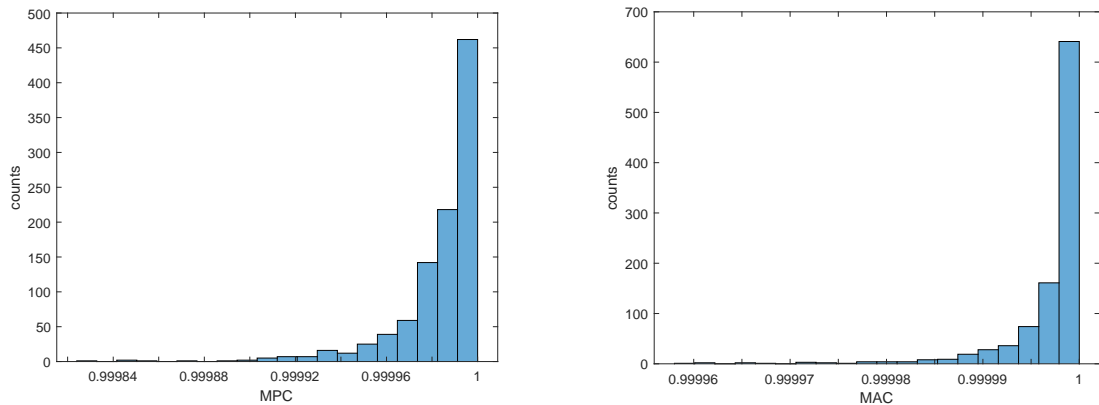


Figure 3: Monte Carlo histogram of $\text{MPC}(\hat{\varphi}^{1,12})$ (left). Monte Carlo histogram of $\text{MAC}(\hat{\varphi}^{1,12}, \hat{\psi}^{1,14})$ (right).

It can be observed that the histograms depicted in Figure 3 illustrate two non-Gaussian distributions of the considered MAC and MPC indicators. In the next section we will present a statistical framework that enables to quantify their variance and to approximate their distributions.

3. UNCERTAINTY QUANTIFICATION OF MAC AND MPC FOR THE REAL-VALUED MODE SHAPES FROM THE STABILIZATION DIAGRAM

Recall from (5) that $\text{MPC}(\varphi) = \text{MAC}(\varphi, \bar{\varphi})$. Based on that, define $g(\varphi, \psi)$ to be a function computing the MAC or MPC indicator evaluated for some given estimates of the mode shape vectors $\hat{\varphi}$ and $\hat{\psi}$. Note that $\psi = \bar{\varphi}$ for the computation of the MPC in $g(\varphi, \psi)$. The first order Taylor expansion of $g(\hat{\varphi}, \hat{\psi})$ writes as

$$g(\hat{\varphi}, \hat{\psi}) = g(\varphi_*, \psi_*) + \mathcal{J}_{\varphi_*, \psi_*}^g \hat{X} + o(\|\hat{X}\|), \quad (6)$$

where $\hat{X} = [\Re(\hat{\varphi} - \varphi_*)^T \quad \Im(\hat{\varphi} - \varphi_*)^T \quad \Re(\hat{\psi} - \psi_*)^T \quad \Im(\hat{\psi} - \psi_*)^T]^T$ and the Jacobian $\mathcal{J}_{\varphi_*, \psi_*}^g$ is expressed as

$$\mathcal{J}_{\varphi_*, \psi_*}^g = \left[\frac{\partial g}{\partial \text{vec}(\Re(\varphi))}(\varphi_*, \psi_*) \quad \frac{\partial g}{\partial \text{vec}(\Im(\varphi))}(\varphi_*, \psi_*) \quad \frac{\partial g}{\partial \text{vec}(\Re(\psi))}(\varphi_*, \psi_*) \quad \frac{\partial g}{\partial \text{vec}(\Im(\psi))}(\varphi_*, \psi_*) \right].$$

A classical approach for the uncertainty quantification of $g(\hat{\varphi}, \hat{\psi})$ is to use a first order perturbation approach and use the first order Delta method to infer its distribution. The first order perturbation of $g(\hat{\varphi}, \hat{\psi})$ can be written as

$$\Delta g(\hat{\varphi}, \hat{\psi}) = \hat{\mathcal{J}}_{\hat{\varphi}, \hat{\psi}}^g \hat{X} \approx \mathcal{J}_{\varphi_*, \psi_*}^g \hat{X}, \quad (7)$$

which assumes that $\mathcal{J}_{\varphi_*, \psi_*}^g$ is a non-zero matrix. Conditions for that are summarized in the following Lemma.

Lemma 1 *The necessary and sufficient conditions for $\mathcal{J}_{\varphi_*, \psi_*}^g \neq 0$ are*

$$\forall \varphi_*, \psi_* \in \mathbb{C}^r \quad \mathcal{J}_{\varphi_*, \psi_*}^g \neq 0 \Leftrightarrow g(\varphi_*, \psi_*) \neq \{0, 1\}.$$

Hence, a first-order perturbation as in (7) is not sufficient to analyse the distribution of the function g for mode shapes that lead to MAC or MPC values of 0 or 1.

Now, consider the case of the MAC and the MPC for estimates of real-valued mode shapes selected from the model alignment a in the stabilization diagram. As such, it can be inferred from Section 2.2. and Section 2.3. that the true value of both indicators satisfies

1. $\text{MAC}(\varphi_*^a, \psi_*^a) = 1$, since both mode shapes correspond the the same mode,
2. $\text{MPC}(\varphi_*^a) = 1$, since the considered mode shape is asymptotically a real-valued vector.

That information, based on Lemma 1, suggests that $\mathcal{J}_{\varphi_*, \psi_*}^g$ is in fact a null matrix for these cases. The second order Taylor expansion of $g(\hat{\varphi}, \hat{\psi})$ can then be written as

$$g(\hat{\varphi}, \hat{\psi}) = g(\varphi_*, \psi_*) + \frac{1}{2} \hat{X}^T \mathbf{H}_{\varphi_*, \psi_*}^g \hat{X} + o(\|\hat{X}\|^2), \quad (8)$$

where $\mathbf{H}_{\varphi_*, \psi_*}^g$ is the Hessian of function g . Recall that $\hat{X}_{\mathcal{N}} = \sqrt{N} \hat{X}$ converges to a Gaussian variable $X_{\mathcal{N}} \sim \mathcal{N}(0, \Sigma_{\varphi_*, \psi_*})$ when N goes to infinity. The asymptotic properties of $g(\hat{\varphi}, \hat{\psi})$ can be expressed as

$$N(g(\hat{\varphi}, \hat{\psi}) - g(\varphi_*, \psi_*)) \approx \frac{1}{2} \hat{X}_{\mathcal{N}}^T \mathbf{H}_{\varphi_*, \psi_*}^g \hat{X}_{\mathcal{N}} \approx \frac{1}{2} X_{\mathcal{N}}^T \mathbf{H}_{\varphi_*, \psi_*}^g X_{\mathcal{N}}, \quad (9)$$

which follows a distribution that can be approximated by a quadratic polynomial of the underlying mode shape vectors. This distribution is complex to determine, but it can be easily approximated. Rewrite (9) as a function $Q(\hat{X}_N)$ such that

$$Q(\hat{X}_N) = \frac{1}{2} \hat{X}_N^T H_{\hat{\varphi}, \hat{\psi}}^g \hat{X}_N \approx \frac{1}{2} X_N^T H_{\varphi_*, \psi_*}^g X_N \approx N(g(\hat{\varphi}, \hat{\psi}) - g(\varphi_*, \psi_*)) . \quad (10)$$

The distribution of $Q(\hat{X}_N)$ can be approximated with a scaled $\chi_{l_{PT}}^2$ distribution with l_{PT} degrees of freedom, after [8], as follows.

Lemma 2 Assume that H_{φ_*, ψ_*}^g is a positive semi-definite matrix. The approximate probability distribution function of $Q(\hat{X}_N)$ writes

$$f_Q(y) = \frac{1}{\alpha} f_{\chi_{l_{PT}}^2} \left(\frac{y - \beta}{\alpha} \right) \quad (11)$$

where $y \in [\beta, +\infty]$ and $f_Q(y) = 0$ for $y < \beta$. The respective scaling and shift parameters of the approximate distribution, α and β , are defined such that $\alpha = \sigma_Q / \sigma_{\chi^2}$ and $\beta = \mu_Q - (\mu_{\chi^2} \sigma_Q) / \sigma_{\chi^2}$. The mean μ_Q and standard deviation σ_Q of the quadratic form are computed using its first cumulants, c_1 and c_2 , namely $\mu_Q = c_1$ and $\sigma_Q = \sqrt{2c_2}$, where the k -th asymptotic cumulant of $Q(\hat{X}_N)$ writes as

$$c_k = \text{tr} \left(\left(\frac{1}{2} H_{\varphi_*, \psi_*}^g \Sigma_{\varphi_*, \psi_*} \right)^k \right) . \quad (12)$$

The mean μ_{χ^2} and standard deviation σ_{χ^2} of the approximating $\chi_{l_{PT}}^2$ distribution are computed from its number of degrees of freedom l_{PT} , such that $\mu_{\chi^2} = l_{PT}$ and $\sigma_{\chi^2} = \sqrt{2l_{PT}}$, where $l_{PT} = c_2^3 / c_3^2$.

The derivation of the expressions for the $\mathcal{J}_{\varphi_*, \psi_*}^g$, H_{φ_*, ψ_*}^g and necessary proofs for Lemma 1 and Lemma 2 are excluded from this paper due to the space limitation.

4. NUMERICAL VALIDATION

This section concludes the developments of this paper by presenting the results of the variance computation of the global MAC and MPC obtained from the stabilization diagram. The global estimates of MAC and MPC are computed for one realization among all the Monte Carlo simulations that corresponds to data set used to establish Figure 1 in Section 2.4.. Here the latter Figure is updated by the estimates of MAC and MPC and their corresponding 95% confidence bounds.

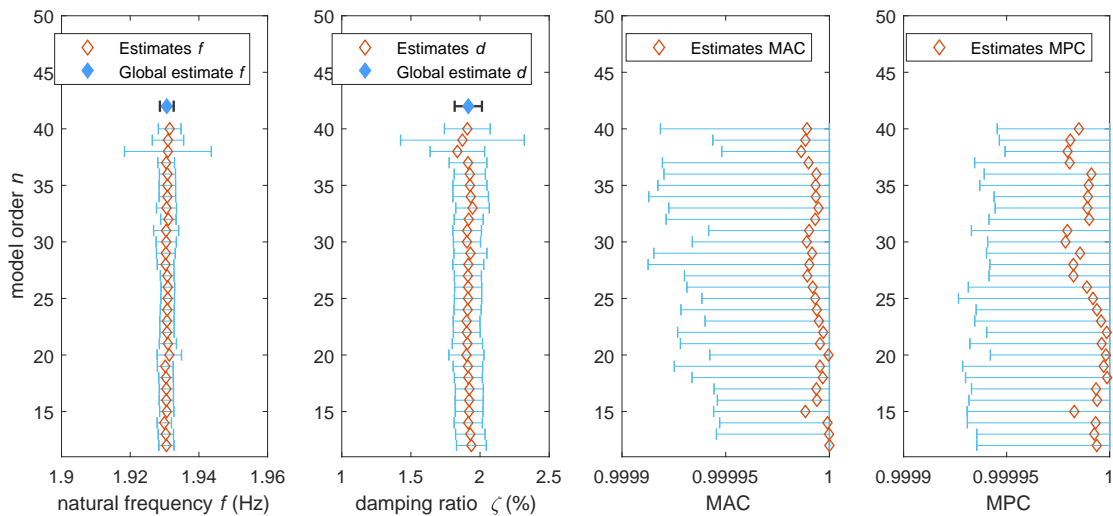


Figure 4: . Estimates of natural frequencies, damping ratios, MAC and MPC from the first modal alignment.

Despite both MAC and MPC being very close to their respective boundaries, their uncertainty can be quantified, as presented on Figure 4. Estimated uncertainties are small however, apart from illustrating the variances in the estimates of the MAC and MPC, the variances of both indicators reflect the underlying variances of the global mode shape estimates.

The quadratic fits to the Monte Carlo histogram from Figure 3 are compared to the classical Gaussian approximation of estimates of the MAC and the MPC based on the first order perturbation theory and Delta method, based on (7).

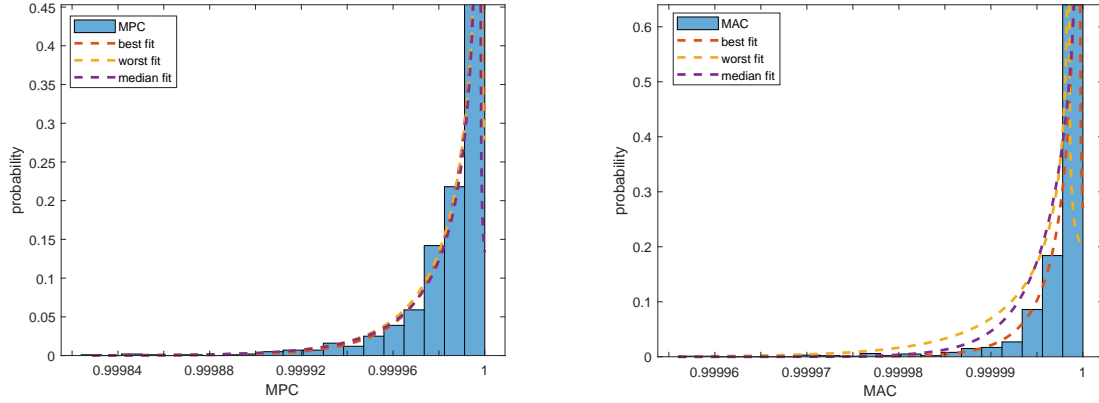


Figure 5: Monte Carlo histogram of $MPC(\hat{\varphi}^{1,12})$ (left). Monte Carlo histogram of $MAC(\hat{\varphi}^{1,12}, \hat{\psi}^{1,14})$ (right). Quadratic fits.

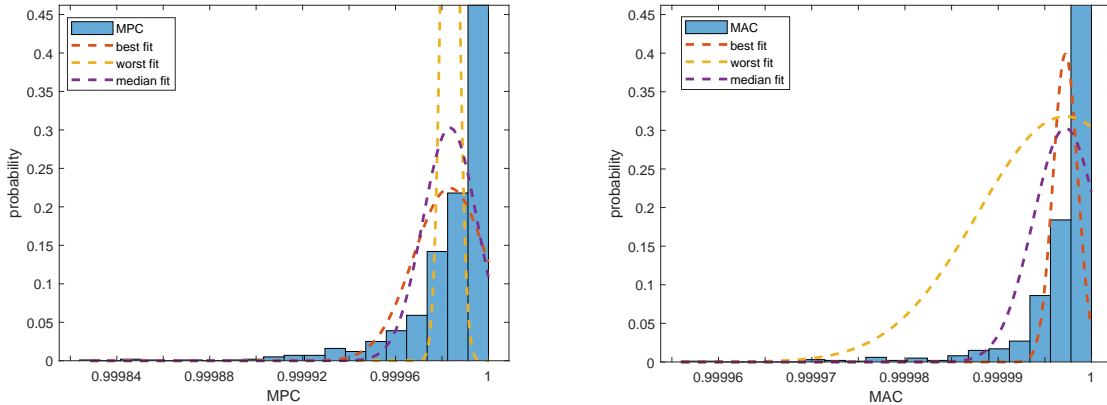


Figure 6: Monte Carlo histogram of $MPC(\hat{\varphi}^{1,12})$ (left). Monte Carlo histogram of $MAC(\hat{\varphi}^{1,12}, \hat{\psi}^{1,14})$ (right). Gaussian fits.

The Gaussian approximation for the distribution of the estimates of the MAC and the MPC obtained from the stabilization diagram is inadequate. Conversely, the quadratic approximation yields accurate fits, as expected. The best, the worst and the median fits presented on Figure 5 and Figure 6 are established based on the statistical properties of the respective distributions computed on one data set and evaluated thanks to a goodness of fit criterion.

5. CONCLUSIONS

In this paper, we have developed a framework for uncertainty quantification of the Modal Assurance Criterion (MAC) and Modal Phase Co-linearity (MPC) for the asymptotically real-valued mode shapes estimated through a stabilization diagram. The proposed scheme allows to accurately compute the variance and approximate the distribution of the aforementioned modal indicators using a quadratic approx-

imation. The resultant framework is more adequate than the classical Gaussian approach for uncertainty quantification, which is illustrated based on numerical simulations.

REFERENCES

- [1] M. Döhler, P. Andersen, and L. Mevel. Variance computation of modal parameter estimates from UPC subspace identification. In *IOMAC - 7th International Operational Modal Analysis Conference*, Ingolstadt, Germany, 2017.
- [2] M. Döhler, F. Hille, L. Mevel, and W. Rucker. Structural health monitoring with statistical methods during progressive damage test of S101 bridge. *Engineering Structures*, 69:183 – 193, 06 2014.
- [3] M. Döhler, X.-B. Lam, and L. Mevel. Uncertainty quantification for modal parameters from stochastic subspace identification on multi-setup measurements. *Mechanical Systems and Signal Processing*, 36:562–581, 04 2013.
- [4] M. Döhler, X.-B. Lam, and L. Mevel. Multi-order covariance computation for estimates in stochastic subspace identification using QR decompositions. *IFAC Proceedings Volumes*, 47(3):9498 – 9503, 2014. 19th IFAC World Congress.
- [5] M. Döhler and L. Mevel. Efficient multi-order uncertainty computation for stochastic subspace identification. *Mechanical Systems and Signal Processing*, 38(2):346–366, 2013.
- [6] R. J. Allemang. The modal assurance criterion (MAC): Twenty years of use and abuse. *Journal of Sound and Vibration*, 37, 01 2003.
- [7] J.-N. Juang and R. S. Pappa. An eigensystem realization algorithm for modal parameter identification and model reduction. *Journal of Guidance, Control, and Dynamics*, 8:620 – 627, 1985.
- [8] H. Liu, Y. Tang, and H. H. Zhang. A new chi-square approximation to the distribution of non-negative definite quadratic forms in non-central normal variables. *Computational Statistics and Data Analysis*, 53(4):853 – 856, 2009.
- [9] P. Mellinger, M. Döhler, and L. Mevel. Variance estimation of modal parameters from output-only and input/output subspace-based system identification. *Journal of Sound and Vibration*, 379(Supplement C):1 – 27, 2016.
- [10] R. Pappa, K. B. Elliott, and A. Schenk. A consistent-mode indicator for the eigensystem realization algorithm. *Journal of Guidance Control and Dynamics*, 16, 09 1993.
- [11] R. Pintelon, P. Guillaume, and J. Schoukens. Uncertainty calculation in (operational) modal analysis. *Mechanical Systems and Signal Processing*, 21(6):2359 – 2373, 2007.
- [12] E. Reynders, K. Maes, G. Lombaert, and G. D. Roeck. Uncertainty quantification in operational modal analysis with stochastic subspace identification: Validation and applications. *Mechanical Systems and Signal Processing*, 66-67:13 – 30, 2016.
- [13] E. Reynders, R. Pintelon, and G. D. Roeck. Uncertainty bounds on modal parameters obtained from stochastic subspace identification. *Mechanical Systems and Signal Processing*, 22(4):948 – 969, 2008. Special Issue: Crack Effects in Rotordynamics.
- [14] P. Vacher, B. Jacquier, and A. Buchardes. Extensions of the mac criterion to complex modes. In *ISMA 2010 International Conference on Noise and Vibration Engineering*, 2010.